



OPEN

## Hydrogen peroxide can be a plausible biomarker in cyanobacterial bloom treatment

Takashi Asaeda<sup>1,2,3✉</sup>, Mizanur Rahman<sup>1</sup> & Helayaye Damitha Lakmali Abeynayaka<sup>1</sup>

The effect of combined stresses, photoinhibition, and nutrient depletion on the oxidative stress of cyanobacteria was measured in laboratory experiments to develop the biomass prediction model. *Phormidium ambiguum* was exposed to various photosynthetically active radiation (PAR) intensities and phosphorous (P) concentrations with fixed nitrogen concentrations. The samples were subjected to stress assays by detecting the hydrogen peroxide (H<sub>2</sub>O<sub>2</sub>) concentration and antioxidant activities of catalase (CAT) and superoxide dismutase (SOD). H<sub>2</sub>O<sub>2</sub> concentrations decreased to 30 μmol m<sup>-2</sup> s<sup>-1</sup> of PAR, then increased with higher PAR intensities. Regarding P concentrations, H<sub>2</sub>O<sub>2</sub> concentrations (nmol L<sup>-1</sup>) generally decreased with increasing P concentrations. SOD and CAT activities were proportionate to the H<sub>2</sub>O<sub>2</sub> protein<sup>-1</sup>. No H<sub>2</sub>O<sub>2</sub> concentrations detected outside cells indicated the biological production of H<sub>2</sub>O<sub>2</sub>, and the accumulated H<sub>2</sub>O<sub>2</sub> concentration inside cells was parameterized with H<sub>2</sub>O<sub>2</sub> concentration protein<sup>-1</sup>. With over 30 μmol m<sup>-2</sup> s<sup>-1</sup> of PAR, H<sub>2</sub>O<sub>2</sub> concentration protein<sup>-1</sup> had a similar increasing trend with PAR intensity, independently of P concentration. Meanwhile, with increasing P concentration, H<sub>2</sub>O<sub>2</sub> protein<sup>-1</sup> decreased in a similar pattern regardless of PAR intensity. Protein content decreased with gradually increasing H<sub>2</sub>O<sub>2</sub> up to 4 nmol H<sub>2</sub>O<sub>2</sub> mg<sup>-1</sup> protein, which provides a threshold to restrict the growth of cyanobacteria. With these results, an empirical formula—protein (mg L<sup>-1</sup>) = -192 \* Log((H<sub>2</sub>O<sub>2</sub>/protein)/4.1), where H<sub>2</sub>O<sub>2</sub>/protein (nmol mg<sup>-1</sup>) = -0.312 \* PAR<sup>2</sup> / (50<sup>2</sup> + PAR<sup>2</sup>) \* ((25/PAR)<sup>4</sup> + 1) \* Log(P/133,100), as a function of total phosphorus concentration, P (μg L<sup>-1</sup>)—was developed to obtain the cyanobacteria biomass.

Cyanobacteria blooms often produce toxic metabolites and are harmful to other organisms as well as humans. Hydrogen peroxide (H<sub>2</sub>O<sub>2</sub>) is often endorsed to reduce cyanobacterial abundance and organic pollutants as it is more effective in application with cyanobacteria compared to other phytoplankton<sup>1,2</sup>. Various experimental approaches have been completed in wastewater treatment, such as advanced oxidation processes, investigation of the degradation of aniline, and evaluation of kenaf fibers and water reservoirs by biological methods<sup>3-6</sup>. However, H<sub>2</sub>O<sub>2</sub> is also produced by other factors. First, H<sub>2</sub>O<sub>2</sub> is generated photochemically from dissolved chromophoric organic materials exposed to UV, and H<sub>2</sub>O<sub>2</sub> distribution was observed in natural lakes<sup>7-9</sup>. At the same time, H<sub>2</sub>O<sub>2</sub> is biologically produced in cells exposed to environmental stresses, including metal ion toxicity, salinization, temperature, PAR conditions, eutrophication, allelopathy, and pathogens. However, its contribution to the total concentration is unknown.

Under a stress environment, endogenous reactive oxygen species (ROS) production, including superoxide, hydroxyl radicals, and H<sub>2</sub>O<sub>2</sub> concentration exceeds its scavenging capacity<sup>10-12</sup>. ROS are essential for growth regulation and signaling mechanisms in photosynthetic organisms<sup>13,14</sup>. Those organisms, in turn, are capable of controlling excess ROS production with their inherent scavenging enzymes and non-enzymatic components<sup>13,15</sup>. Accumulation of excessive ROS inside cells causes harmful impacts on cyanobacteria, such as disrupting cellular homeostasis, causing membrane lipid peroxidation, protein oxidation, enzyme inhibition, and DNA and RNA damages. It also affects the photosynthetic apparatus, leading to cell mortality as the concentration exceeds the threshold value<sup>16</sup>.

Cyanobacteria are sensitive to even a minor change in light intensity as they usually expose relatively weak light; thus, even moderate solar radiation may cause stress<sup>17</sup>. The collection of solar energy at photosystem II (PSII) in the thylakoid membrane results in the oxidation of water molecules and reduction of plastoquinone, a molecule involved in the electron transport chain. The produced electrons are transported to PSI, where they are consumed in the synthesis of carbohydrates. However, an overabundance of solar energy results in the generation

<sup>1</sup>Saitama University, Saitama 338-8570, Japan. <sup>2</sup>Hydro Technology Institute, Shimo-meguro, Tokyo, Japan. <sup>3</sup>Research and Development Center, Nippon Koei, Tsukuba, Japan. ✉email: asaeda@mail.saitama-u.ac.jp

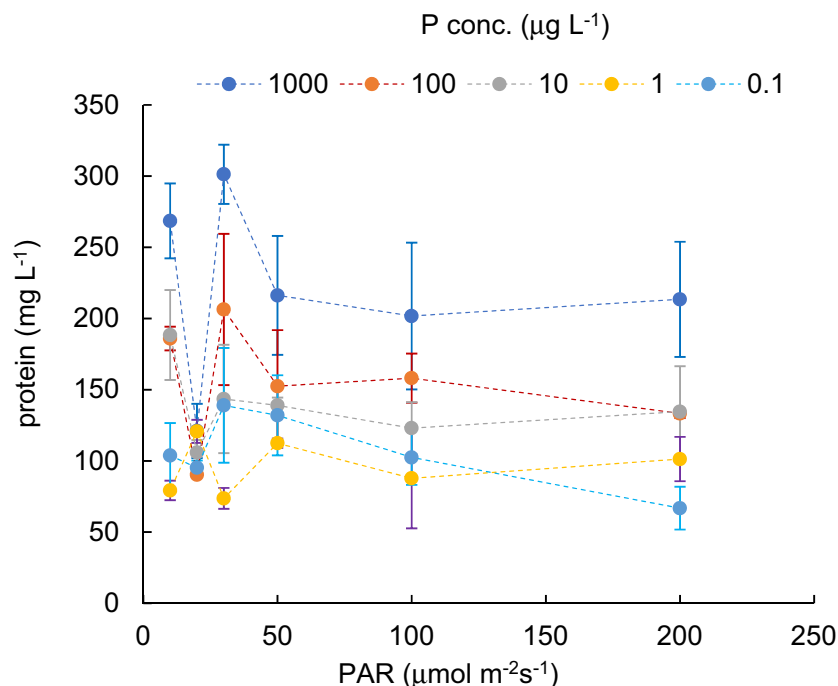


**Figure 1.** Protein content for different PAR intensity levels and for each phosphorus concentration level. Vertical bars indicate standard deviation.

of ROS, including superoxide radicals, as the energy transfer rate is limited due to the underutilization of energy absorbed by the PSII antenna complex in the PSII reaction center<sup>15,18–20</sup>. Superoxide dismutase (SOD) catalyzes superoxide radicals into H<sub>2</sub>O<sub>2</sub> before being detoxified into water by antioxidant activities<sup>21</sup>. However, the high oxidation potential of ROS can lead to the destruction of proteins, which otherwise recover the photosystem activities<sup>22</sup>. Thus, excessive solar radiation inhibits the proliferation of cyanobacteria. Similarly, the shortage of nutrient conditions, including P and nitrogen (N), is identified as a dominant stressor that suppresses the growth of cyanobacteria<sup>23</sup>. P is an important macronutrient to plankton growth in many ways. It makes rigid structures in cell walls, membranes, and nucleic acids by making covalent links between monomers. It is also involved in cell metabolism directly by storing energy as polyphosphate bodies in plankton cells<sup>24</sup>. The absolute concentrations of P and N and the stoichiometric ratio of these elements often play an important role in plankton growth in lakes<sup>25</sup>. N:P mass ratio varies between 240 and 0.5, depending on the variation of P concentration in lakes<sup>26</sup>. When the mass ratio of N:P exceeds 10, P is considered as the limiting factor. On the other hand, when N:P less than 10, N becomes the limiting factor on phytoplankton growth, including cyanobacteria in freshwater bodies<sup>27</sup>. Hence, both surplus and deficiency of nutrients could cause significant alternations in cyanobacteria biomass and cellular stress. The combined effect of various abiotic stresses on the production rate is often reported<sup>28,29</sup>. Some combinations inhibit growth due to the contradicting impacts of stressors; however, a significant reduction of biomass is also reported as caused by simultaneous exposure to multiple stressors compared to a single stress source<sup>30</sup>. Hence, excessive radiation stress combined with a shortage of P and N nutrients could generate huge cellular stress and cyanobacterial growth inhibition.

The concentration of H<sub>2</sub>O<sub>2</sub> and the activity of antioxidant enzymes are some of the biomarkers employed in stress detections. The role of H<sub>2</sub>O<sub>2</sub> in plants and how they respond to environmental stress has been a focus throughout the literature<sup>31–33</sup>, suggesting a potential to develop ROS-based strategies for predicting cyanobacterial bloom formation and H<sub>2</sub>O<sub>2</sub> concentrations<sup>34</sup>. Thus, this research was designed to study the (1) effects of the PAR regime and P concentrations on cyanobacteria stress, particularly endogenous H<sub>2</sub>O<sub>2</sub> concentrations, under the condition of naturally produced H<sub>2</sub>O<sub>2</sub> from organic matter, (2) combined effects of the PAR regime and P concentrations on H<sub>2</sub>O<sub>2</sub> concentrations, and (3) relationship between H<sub>2</sub>O<sub>2</sub> concentrations and antioxidant enzyme activities of cyanobacteria, aiming at the possibility of applying H<sub>2</sub>O<sub>2</sub> concentrations as a proxy to detect stress intensity in algal management and the contribution rate of the biological H<sub>2</sub>O<sub>2</sub> production rate in the treatment.

## Results

**The effect of PAR intensity and phosphorous concentration on H<sub>2</sub>O<sub>2</sub> concentration.** Variations in protein contents of cyanobacterial cultures (mg L<sup>-1</sup>), grown under different PAR intensity levels with different P concentrations, are shown in Fig. 1. Figure 2 indicates the H<sub>2</sub>O<sub>2</sub> concentration variations (nmol L<sup>-1</sup>) for different PAR intensity levels and each P concentration level. Vertical bars indicate standard deviation. Higher protein content was obtained when PAR exposure was lower than 50 μmol m<sup>-2</sup> s<sup>-1</sup>. In a PAR intensity range between 0 and 30 μmol m<sup>-2</sup> s<sup>-1</sup>, the H<sub>2</sub>O<sub>2</sub> concentration declined from 50 to 150 nmol L<sup>-1</sup> at dark condition, with increasing PAR. With a PAR intensity between a 30 and 200 μmol m<sup>-2</sup> s<sup>-1</sup> range, the protein content was

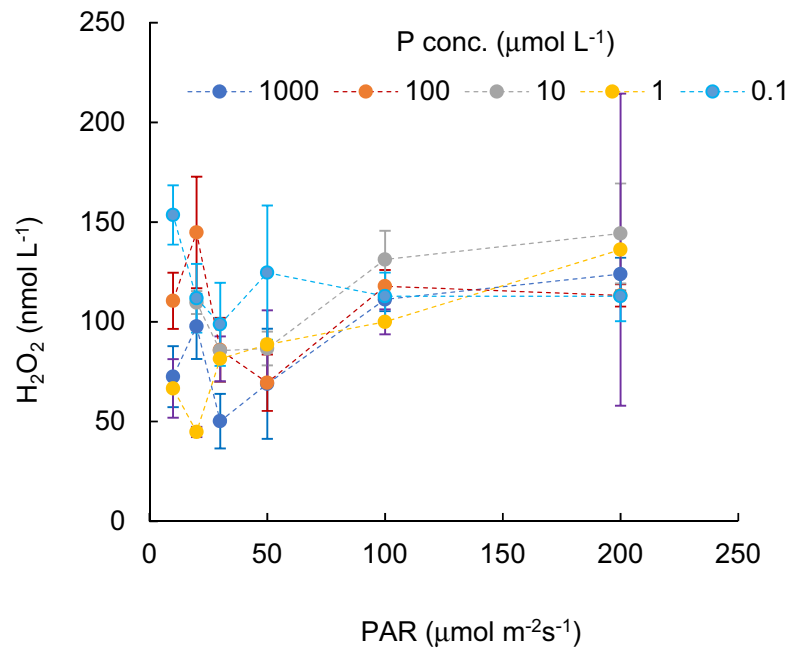


**Figure 2.**  $\text{H}_2\text{O}_2$  concentration for different PAR intensity levels and for each phosphorus concentration level. Vertical bars indicate standard deviation.

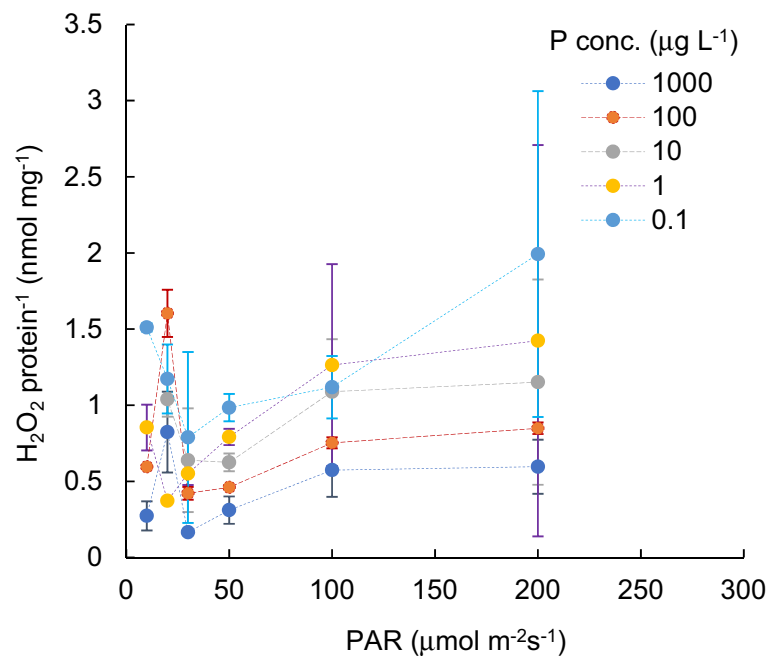


**Figure 3.**  $\text{H}_2\text{O}_2$  content per protein for different PAR intensity levels and for each P concentration level. Vertical bars indicate standard deviation.

slightly reduced ( $R^2 = -0.06$ ,  $p > 0.1$ ), while the  $\text{H}_2\text{O}_2$  concentration significantly increased ( $R^2 = 0.73$ ,  $p < 0.001$ , and 0.910, 0.720, 0.92, 0.92 and 0.16 for 1000, 100, 10, 1.0, 0.1  $\mu\text{g L}^{-1}$  of P concentration, respectively), regardless of the P concentration. The variational trend of  $\text{H}_2\text{O}_2$  concentration per protein ( $\text{nmol mg}^{-1}$ ) is shown in Fig. 3 with respect to the PAR intensity. Regardless of the P concentration, it declined with low PAR intensities to  $30 \mu\text{mol m}^{-2} \text{s}^{-1}$  of PAR intensity and then increased with a decreasing enhancement rate. At values higher than  $50 \mu\text{mol m}^{-2} \text{s}^{-1}$  PAR, no significant difference was obtained in the variational trend of the  $\text{H}_2\text{O}_2$  per protein with respect to PAR. The increasing trend of  $\text{H}_2\text{O}_2$  per protein with PAR intensity is mainly attributed to the increasing trend of  $\text{H}_2\text{O}_2$  concentration rather than the reduction of protein content.  $\text{H}_2\text{O}_2$  per protein was generally lower with a higher P concentration ( $p < 0.03$ ).  $\text{H}_2\text{O}_2$  per protein, measured as high as 0.2 up to  $2.0 \text{ nmol mg}^{-1}$

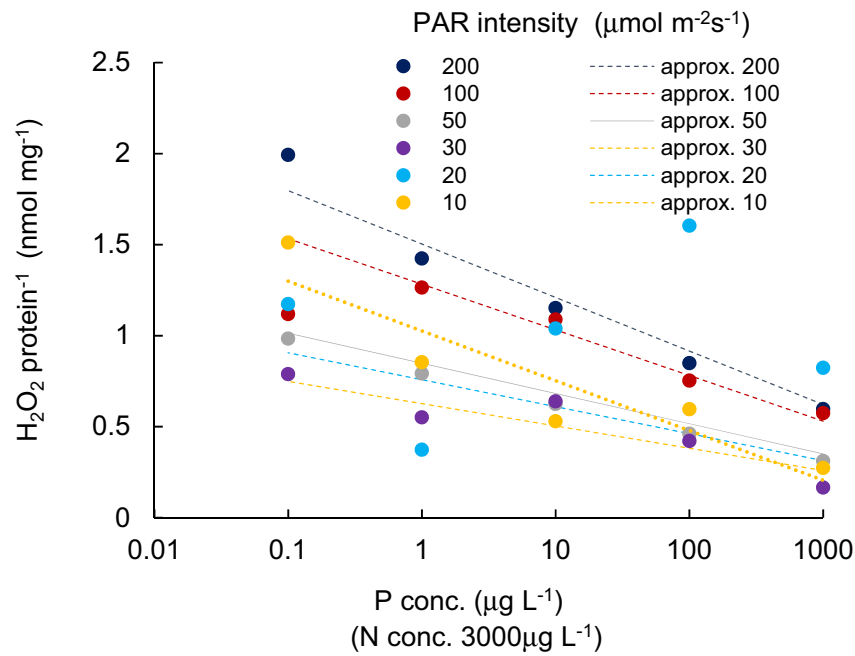


**Figure 4.**  $\text{H}_2\text{O}_2$  content per protein for different P concentration level and for each PAR intensity level. Vertical bars indicate standard deviation. Dotted lines show the approximate relation for each light intensity.

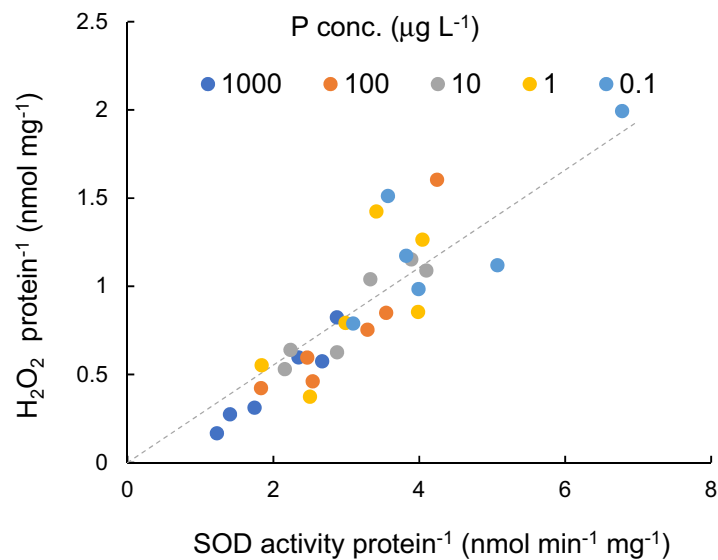


**Figure 5.** Relation between SOD activity and  $\text{H}_2\text{O}_2$  concentration for different P concentration level. The approximate relation is shown by the diagonal line.

with 10–200  $\mu\text{mol m}^{-2} \text{s}^{-1}$  of PAR intensities, declined with a higher P concentration uniquely except for 20  $\mu\text{mol m}^{-2} \text{s}^{-1}$  (Fig. 4).

**Antioxidant activities with respect to  $\text{H}_2\text{O}_2$  concentration per protein.** SOD activity per protein was uniquely proportionate to  $\text{H}_2\text{O}_2$  per protein (Fig. 5). The approximate relation is shown by the diagonal line, where the  $\text{H}_2\text{O}_2 \text{ protein}^{-1} (\text{nmol mg}^{-1}) = 0.276(\text{min}) * \text{SOD} (\text{nmol mg}^{-1} \text{min}^{-1})$ , ( $R^2 = 0.950$ ,  $p < 0.01$ ).

CAT activity per protein is shown as a function of  $\text{H}_2\text{O}_2$  concentration per protein, separately shown by each P concentration in Fig. 6. For each P concentration level, CAT activity per protein linearly increased with the  $\text{H}_2\text{O}_2 \text{ protein}^{-1}$ . The increasing rate was higher based on PAR intensity (18.73 CAT  $\text{H}_2\text{O}_2^{-1}$ ,  $R^2 = 0.573$  for 1000  $\mu\text{g L}^{-1}$ , 13.82 CAT  $\text{H}_2\text{O}_2^{-1}$ ,  $R^2 = 0.977$  for 100  $\mu\text{g L}^{-1}$ ; 12.89 CAT  $\text{H}_2\text{O}_2^{-1}$ ,  $R^2 = 0.793$  for 10  $\mu\text{g L}^{-1}$ ; 14.53 CAT  $\text{H}_2\text{O}_2^{-1}$ ,  $R^2 = 0.949$  for 1  $\mu\text{g L}^{-1}$ ; and 9.22 CAT  $\text{H}_2\text{O}_2^{-1}$ ,  $R^2 = 0.766$ , for 0.1  $\mu\text{g L}^{-1}$ ), and the proportional

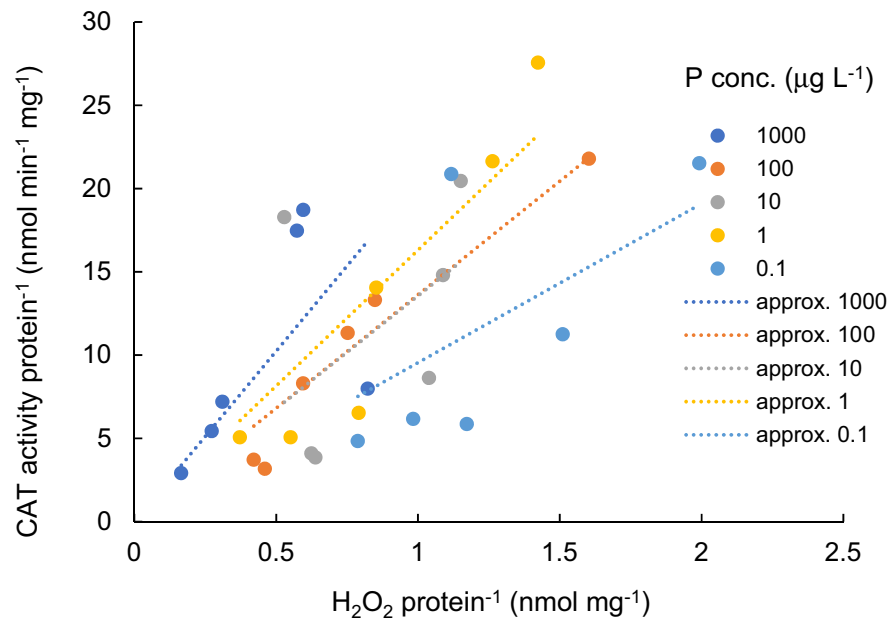


**Figure 6.** Relation between H<sub>2</sub>O<sub>2</sub> concentration and CAT activity for different P concentration levels. Dotted lines indicate the approximate lines for each P concentration.

coefficient was found to have a significant positive correlation with the logarithmic scale of the P concentration ( $p < 0.01$ ).

On the other hand, for each PAR intensity level, CAT activity did not have significant positive correlation with the P concentration level.

## Discussion

**The effect of biologically produced H<sub>2</sub>O<sub>2</sub> on the suppression of cyanobacterial blooms.** The artificial endorsement of H<sub>2</sub>O<sub>2</sub> has a high potential to suppress cyanobacterial blooms with less effect on other organisms compared to other controlling methods<sup>35–39</sup>. Previous researchers obtained the lethal H<sub>2</sub>O<sub>2</sub> dosage for cyanobacteria by laboratory incubations under different H<sub>2</sub>O<sub>2</sub> concentrations; cyanobacterial chlorophyll declined to nearly half after an 18 h incubation with approximately 30 µmol L<sup>-1</sup> of H<sub>2</sub>O<sub>2</sub><sup>1,40</sup> or after a 4 h incubation with 100 µmol L<sup>-1</sup> of H<sub>2</sub>O<sub>2</sub><sup>2</sup>. H<sub>2</sub>O<sub>2</sub> delayed fluorescence decay with 0.1 µmol of H<sub>2</sub>O<sub>2</sub> L<sup>-17</sup>. At the same time, the Fv/Fm value substantially declined with 100 µmol of H<sub>2</sub>O<sub>2</sub> L<sup>-141</sup>, and dead cells increased with 275 µmol of H<sub>2</sub>O<sub>2</sub> L<sup>-139</sup>. Cyanobacteria were in a lethal condition<sup>1,2</sup> and sub-lethal at concentrations exceeding 50 µmol of H<sub>2</sub>O<sub>2</sub> L<sup>-139</sup>. All previous experimental results reveal that cyanobacterial biomass is degraded with higher H<sub>2</sub>O<sub>2</sub> concentrations; however, the H<sub>2</sub>O<sub>2</sub> concentration threshold varies widely from 1 to 1000 µmol L<sup>-1</sup>. In the present study, we used protein content as an indicator of biomass rather than the chlorophyll content of *Phormidium ambiguum* cells because chlorophyll-a can be expressed on a protein basis<sup>42</sup>. However, the decreasing trend of protein content, which was seen with the Chl-a concentration, was also observed with H<sub>2</sub>O<sub>2</sub> concentrations.

Natural H<sub>2</sub>O<sub>2</sub> formation has been identified in aquatic ecosystems as photolysis of dissolved organic carbon (DOC) exposed to UV<sup>7,43,44</sup>. Then it is reported that the H<sub>2</sub>O<sub>2</sub> production varies with the nutrient content of the water body. However, the H<sub>2</sub>O<sub>2</sub> concentration of these waters was in the magnitude of µmol L<sup>-18,34,45</sup>. The comparison of these results indicates that the photolysis of organic carbon in natural water only is not sufficient to control cyanobacterial biomass.

H<sub>2</sub>O<sub>2</sub> is also produced biologically and is accumulated in cells subject to high levels of environmental stress. In the present study, UV was limited. Accordingly, measured H<sub>2</sub>O<sub>2</sub> was considered a biologically produced component in cells or cell surfaces, which was then released into the ambient water. In the present experiment, protein content was measured as a reference of the biomass of cyanobacteria. Cell biomass is two to three times larger with protein content<sup>46</sup>.

As the buoyancy of the cells is nearly neutral, the H<sub>2</sub>O<sub>2</sub> content per protein, ~ 1 mmol of H<sub>2</sub>O<sub>2</sub> kg<sup>-1</sup>, was generated and contained in the cell before release. This constitutes more or less the same level of the lethal H<sub>2</sub>O<sub>2</sub> concentration in water.

The protein content in water declined with an increasing H<sub>2</sub>O<sub>2</sub> concentration per protein up to 2 nmol mg<sup>-1</sup> protein (Fig. 7). It was nearly same as the lethal level of the previous studies<sup>35,39</sup>. A higher protein level was not observed with higher H<sub>2</sub>O<sub>2</sub> concentration levels in the present study. The growth of cyanobacteria is suppressed by the generation of higher H<sub>2</sub>O<sub>2</sub> levels.

The lethal H<sub>2</sub>O<sub>2</sub> concentration obtained here corresponds well with about 16 µmol of H<sub>2</sub>O<sub>2</sub> g<sup>-1</sup> FW of a threshold condition to grow *Egeria densa* in natural water<sup>33</sup>, considering the weakness of cyanobacteria to H<sub>2</sub>O<sub>2</sub> rather than other plant species<sup>35</sup>.

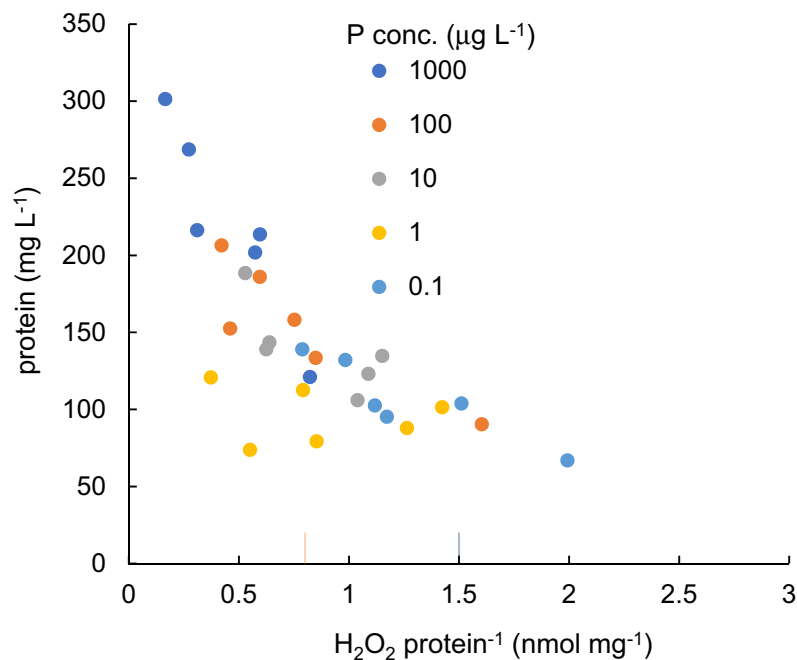


**Figure 7.** Relation between  $\text{H}_2\text{O}_2$  concentration per protein and protein content in water for different P concentration levels. Lethal level of cyanobacteria in the previous reports<sup>35,39</sup> are shown for comparison.

**The possible indicator of environmental stress and the effect of combined stress factors.** The accumulation of ROS is reported to augment in parallel fashion to increased abiotic stress<sup>47–49</sup>. In the present experiment, two types of abiotic stresses, phosphorous deficiency and high or low PAR intensities, were applied with different intensities of each.

Though  $\text{H}_2\text{O}_2$  is produced under normal environmental conditions, its production is accelerated under high stress intensity. In natural water, cyanobacteria often suffer from a shortage of N and P. Stoichiometrically, the ratio of the N and P of cyanobacterial cells is approximately 16:1<sup>50</sup>. Waters with an N:P ratio of < 15 are most susceptible to cyanobacterial dominance<sup>51,52</sup>. In the present experiment, the P concentration was changed with the fixed amount of an N concentration of 3000  $\mu\text{g L}^{-1}$ . Thus, the P concentration becomes restrictive, except for 1000  $\mu\text{g L}^{-1}$  in the present study's conditions. A significant increasing trend was observed in  $\text{H}_2\text{O}_2$  per protein with a decreasing P concentration. The deficiency of essential nutrients may increase oxidative stress and then deteriorate the growth rate of cyanobacteria.

Under all tested P concentrations,  $\text{H}_2\text{O}_2$  per protein content decreased with increasing PAR intensity until 30  $\mu\text{mol m}^{-2} \text{s}^{-1}$ , taking the lowest value there, then grew at higher PAR intensities, though the increasing rate gradually decreased. The enhanced production of  $\text{H}_2\text{O}_2$  under prolonged low PAR conditions has not been sufficiently studied, though superoxide production in dark conditions is reported<sup>26</sup>. With submerged macrophytes, *Egeria densa*, the  $\text{H}_2\text{O}_2$  concentration was the lowest empirically under the prolonged exposure of a PAR intensity level of approximately 60  $\mu\text{mol m}^{-2} \text{s}^{-1}$ <sup>133,53</sup>. The  $\text{H}_2\text{O}_2$  concentration increased both with decreasing or increasing PAR intensities. However, the underlying mechanisms are unknown.

The increasing  $\text{H}_2\text{O}_2$  concentration per protein over 30  $\mu\text{mol m}^{-2} \text{s}^{-1}$  of PAR intensity is attributed to the excessive harvesting of PAR energy<sup>17,18</sup>. In the thylakoid membrane, electrons are produced by solar energy and transmitted to plastoquinone in PSII, which are partially accepted for carbon dioxide fixation. More electrons are generated when exposed to higher levels of solar radiation. Consequently, the photoinhibition of photosystem-II (PS-II) is induced, leading to oxidative damage because of the generated ROS such as superoxide, hydroxyl radicals, and  $\text{H}_2\text{O}_2$ . It damages cellular components, such as the D1 protein, which otherwise mends the damaged photosynthesis apparatus<sup>18</sup>.

The process comprises the direct reduction of  $\text{O}_2$  by PS-I, resulting in singlet oxygen production followed by superoxide, which is converted to  $\text{H}_2\text{O}_2$  by the activities of the enzyme SOD. In the present study,  $\text{H}_2\text{O}_2$  per protein was proportionate with SOD activity, generating  $\text{H}_2\text{O}_2$  from superoxide. CAT activity was far higher than other major antioxidant activities to decompose  $\text{H}_2\text{O}_2$  and linearly increased with  $\text{H}_2\text{O}_2$  concentration.

Though SOD and CAT activities demonstrated different dependencies on PAR intensity levels and the P concentration, their activities were evaluated by the single function with  $\text{H}_2\text{O}_2$  per protein. A steady  $\text{H}_2\text{O}_2$  concentration is sustained by balancing the generated  $\text{H}_2\text{O}_2$  with different types of stresses and these antioxidant activities as a single function of  $\text{H}_2\text{O}_2$  content per protein.

In natural water, cyanobacteria are exposed to various abiotic stresses that enhance oxidative stress, producing  $\text{H}_2\text{O}_2$ , which may deteriorate cyanobacterial biomass. A significant negative correlation was recognized for protein content with respect to the  $\text{H}_2\text{O}_2$  concentration ( $n = 90$ ,  $R^2 = -0.712$ ,  $p < 0.01$ ), irrespective of stress types.

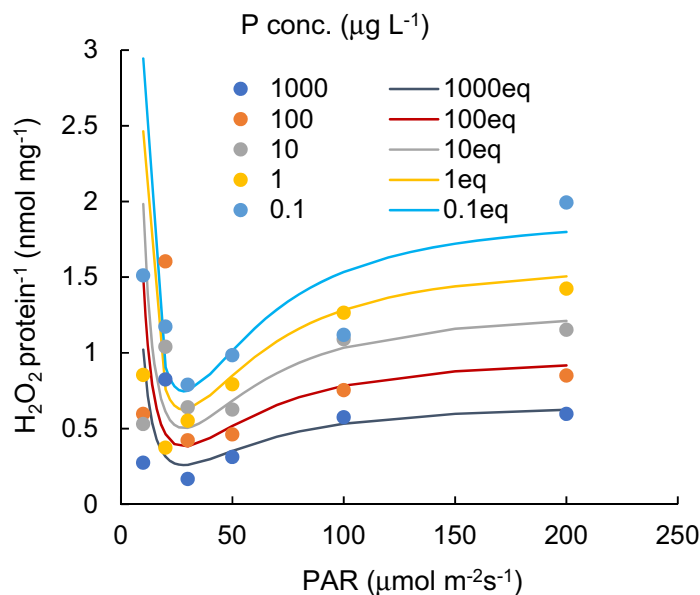


**Figure 8.** The simulated results of  $\text{H}_2\text{O}_2/\text{protein}$  by Eq. (1) compared with experimental results.

The production rate of  $\text{H}_2\text{O}_2$  is not necessarily cumulative for different types of abiotic stresses<sup>28,30</sup>. However, the  $\text{H}_2\text{O}_2$  concentration was enhanced with increasing PAR intensity and decreasing phosphorus concentration, respectively, and the enhancement of the  $\text{H}_2\text{O}_2$  concentration was independent of each other ( $p < 0.01$ ). The total  $\text{H}_2\text{O}_2$  per protein is empirically given as the sum of  $\text{H}_2\text{O}_2$  produced by the intensity of each stress component at least as a practical use level. Thus, the total  $\text{H}_2\text{O}_2$  concentration is approximately provided by the sum of the  $\text{H}_2\text{O}_2$  concentration attributed to each stress. The same trend was obtained for submerged macrophytes<sup>33,53</sup>. Consequently, a potential for using the  $\text{H}_2\text{O}_2$  concentration to estimate cyanobacterial biomass exists.

**The estimation of  $\text{H}_2\text{O}_2$  concentrations produced by cyanobacteria under abiotic stresses.** For the application of the empirically obtained results to practical use in the prediction of algal blooms in the environment where PAR and P concentrations are restricted factors for growth, the trend of the  $\text{H}_2\text{O}_2$  per protein ( $\text{nmol mg}^{-1}$ ) is obtained as a function of PAR ( $\mu\text{mol m}^{-2} \text{s}^{-1}$ ) and the P concentration, P ( $\mu\text{g L}^{-1}$ ), as formulated by:

$$\text{H}_2\text{O}_2/\text{protein} = -0.312 * \text{PAR}^2 / (50^2 + \text{PAR}^2) * ((25/\text{PAR})^4 + 1) * \text{Log}(P/133,100) \quad (1)$$

where  $0.1 \mu\text{g PL}^{-1} < P < 1000 \mu\text{g PL}^{-1}$ ,  $30 \mu\text{mol m}^{-2} \text{s}^{-1} < \text{PAR}$ , and protein represents the amount of protein in  $\text{mg L}^{-1}$ .

The relationship is shown in Fig. 8. The simulated results of the  $\text{H}_2\text{O}_2 \text{ protein}^{-1}$  by Eq. (1) compared with experimental results and a significant similarity was obtained ( $R^2 = 0.953$ ,  $p = 0.012$ , for  $1000 \mu\text{g L}^{-1}$ ,  $R^2 = 0.696$ ,  $p = 0.0065$  for  $100 \mu\text{g L}^{-1}$ ;  $R^2 = 0.927$ ,  $p = 0.023$  for  $10 \mu\text{g L}^{-1}$ ;  $R^2 = 0.982$ ,  $p = 0.00289$  for  $1 \mu\text{g L}^{-1}$ ;  $R^2 = 0.024$ , and  $p = 0.024$  for  $0.1 \mu\text{g L}^{-1}$ ).

The protein content ( $\text{mg L}^{-1}$ ) is shown in Fig. 9. The simulated results of protein content by Eq. (2), as a function of  $\text{H}_2\text{O}_2$  per protein, was shown to possess significant negative correlation ( $R^2 = -0.675$ ,  $p < 0.01$ ), which is empirically formulated by:

$$\text{protein} = -192 * \text{Log}((\text{H}_2\text{O}_2/\text{protein})/4.1) \quad (2)$$

( $R^2 = -0.71$ ,  $p < 0.01$ ).

With Eqs. (1) and (2), protein content is estimated as a function of PAR and the P concentration.

The estimated protein contents are denoted in Fig. 9. Protein content in water for different P concentration levels ( $\text{mg L}^{-1}$ ) and for each PAR intensity level ( $\mu\text{mol m}^{-2} \text{s}^{-1}$ ). The concentration uniquely increased with increasing P concentrations.

The cellular growth rate gradually decreased with light intensity<sup>54</sup>, and the growth rate of cyanobacteria reached a maximum at  $30\text{--}50 \mu\text{mol m}^{-2} \text{s}^{-1}$ <sup>55</sup>. *P. ambiguum* prefers relatively low light intensity at  $\sim 18 \mu\text{mol m}^{-2} \text{s}^{-1}$ <sup>56</sup>. The diagram seems to provide reasonable results.

## Conclusions

The endogenous  $\text{H}_2\text{O}_2$  concentration is an effective tool to detect the stress level of cyanobacteria. Both PAR regimes and P concentration shortages are shown to enhance  $\text{H}_2\text{O}_2$  concentrations in cyanobacterial cultures.

$\text{H}_2\text{O}_2$  per protein content declines in low PAR conditions and increases when exposed to higher PAR intensity levels while generally increasing as the P concentration decreases.  $\text{H}_2\text{O}_2$  per protein for combined stresses



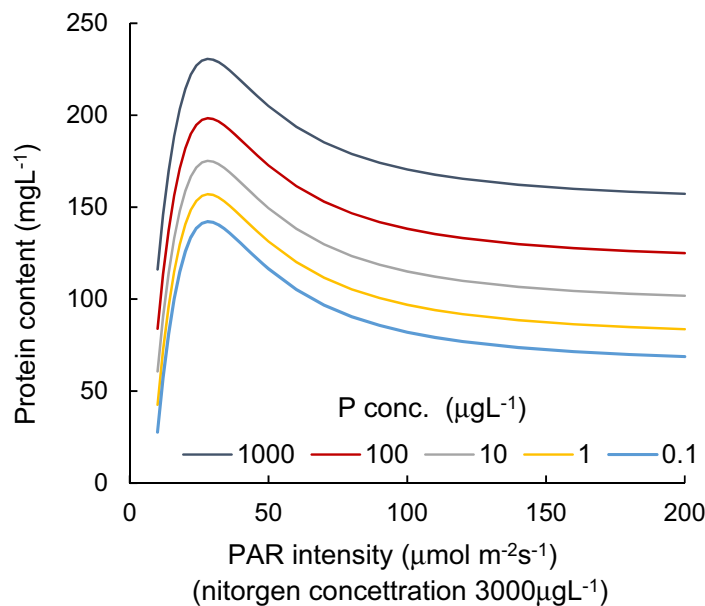


**Figure 9.** The simulated results of protein content.

is given by the sum of the amount produced by each stress. Protein content decreases uniquely following the value of  $H_2O_2$  per protein in a cyanobacterial culture. Then the  $H_2O_2$  per protein exceeds the threshold value, cyanobacteria will decline. As a result, cyanobacterial cell will lyse leading to death. Cyanobacterial cell biomass can easily be regulated by this way.

The prediction model was developed for the protein content to design management criteria for excessive cyanobacterial blooms in freshwaters.

**Methodology.** *Culture and incubation.* *Phormidium ambiguum*, an odor-forming benthic cyanobacterial species, was obtained from the National Institute of Studies (NIES), Japan. The strain was cultured and acclimatized for 30 days in an autoclaved BG 11 medium<sup>57</sup>, maintained at 20 °C under controlled PAR conditions with white fluorescent light, having flux of 20  $\mu\text{mol m}^{-2}\text{s}^{-1}$  in a light-and-dark cycle of 12 h:12 h. The cultures were manually shaken twice a day. Cells were subcultured by diluting with new BG 11 medium as needed.

**Experimental procedure.** After 30 days, well-grown cyanobacterial cells were collected by centrifugation, washed once with distilled water, and then re-suspended in modified BG 11 media. All experiments were conducted by using incubators (MIR-254, Sanyo, Tokyo, Japan) with a nutrient level of BG-11 medium consisting of  $\text{NaNO}_3$  17.6 mM,  $\text{K}_2\text{HPO}_4$  0.2296 mM,  $\text{MgSO}_4 \cdot 7\text{H}_2\text{O}$  0.0146  $\mu\text{M}$ ,  $\text{Na}_2\text{CO}_3$  0.0189  $\mu\text{M}$ , Citric acid 0.0031  $\mu\text{M}$ , Ferric ammonium citrate 0.0023  $\mu\text{M}$ , EDTA ( $\text{Na}_2$  salt) 0.0297  $\mu\text{M}$ ,  $\text{H}_3\text{BO}_3$  4.6253  $\mu\text{M}$ ,  $\text{MnCl}_2 \cdot 4\text{H}_2\text{O}$  0.9145  $\mu\text{M}$ ,  $\text{ZnSO}_4 \cdot 7\text{H}_2\text{O}$  0.0765  $\mu\text{M}$ ,  $\text{Na}_2\text{MoO}_4 \cdot 2\text{H}_2\text{O}$  0.1611  $\mu\text{M}$ ,  $\text{CuSO}_4 \cdot 5\text{H}_2\text{O}$  0.0316  $\mu\text{M}$ , and  $\text{Co}(\text{NO}_3)_2 \cdot 6\text{H}_2\text{O}$  0.0023  $\mu\text{M}$  in 1 L of deionized water<sup>58</sup>, adjusted for N and P concentrations, respectively, at 3000  $\mu\text{g L}^{-1}$  of nitrogen and 0.1, 1.0, 10, 100, and 1000  $\mu\text{g L}^{-1}$  of P. Six different PAR intensities—namely, 10, 20, 30, 50, 100 and 200  $\mu\text{mol m}^{-2}\text{s}^{-1}$ —by white fluorescent light (Toshiba, Japan) and VBP-L24-C2 PAR source (Valore, Kyoto, Japan) were used with 12 h:12 h PAR and dark cycle. The PAR intensities were measured using a quantum sensor (EKO Instruments Co., Ltd., Japan) and adjusted uniformly in the media. The temperature was kept constant (20 °C) throughout the experiment. At 12:00, after 7 days, samples were taken for the subsequent stress response analysis. Collected samples were subjected to bioassays that are described later.

**Analyses.** *Total soluble protein content analysis.* Total soluble protein concentration was determined using the same method mentioned in<sup>57</sup> with minor modifications. Cyanobacterial cells were extracted from 1 mL of culture media by centrifugation at 4 °C for 10 min at 10,000 rpm, and the pellet was washed once with distilled water. Then, the cell pellet was subjected to a freeze–thaw cycle. Total soluble protein was extracted using a 0.5 M NaOH solution, and the extraction was centrifuged at 4 °C for 20 min at 10,000 rpm. The supernatant was used as crude protein extract, and the protein content was quantitatively analyzed with the aid of a Coomassie Bradford protein assay kit. Crude protein extract was stained with Coomassie (G-250) dye and incubated for 10 min at room temperature, and then the absorbance was measured at 595 nm using a UV–Vis spectrometer (Shimazu, Japan). Protein content was determined using a known concentration series of Albumin.

**Stress assay.**  *$H_2O_2$  assay.* Cellular  $H_2O_2$  contents were estimated according to the titanium chloride method<sup>59</sup>. A total of 750  $\mu\text{L}$  of 0.1% titanium chloride in 20%  $\text{H}_2\text{SO}_4$  (v/v) was then added to initiate the reaction. The optical absorption after 1 min was measured at 410 nm using a spectrophotometer (UVmini-1240).



However, the absorption at 410 nm includes the effect of other soluble compounds<sup>60–62</sup>. Thus, the H<sub>2</sub>O<sub>2</sub> concentration was calculated from the slopes of the standard curve obtained from known H<sub>2</sub>O<sub>2</sub> concentrations, which was offset derived by the intercept absorption rate with zero H<sub>2</sub>O<sub>2</sub> concentration samples<sup>61</sup>. The results were compared with those of the e-FOX method and a suitable agreement was obtained<sup>62</sup>.

**CAT assay.** The CAT activity was measured by reacting 15 µL of 750 mM H<sub>2</sub>O<sub>2</sub>, 920 µL of potassium phosphate buffer, and 65 µL of extract supernatant. Optical absorption was measured at 240 nm using UV mini-1240. The measurements were recorded every 20 s for 3 min, and CAT activity was calculated using an extinction coefficient of 39.4 mM<sup>-1</sup> cm<sup>63</sup>. The scavenging rate of H<sub>2</sub>O<sub>2</sub> by enzyme extract per minute was defined as unit of CAT activity per mg of total soluble protein.

**APX assay.** For the APX assay, the reaction mixture contained 100 µL of enzyme extract, 200 µL of 0.5 mM ascorbic acid in 50 mM potassium phosphate buffer (pH 7.0), and 2 mL of 50 mM potassium phosphate buffer (pH 7.0) mixed with 60 µL of 1 mM H<sub>2</sub>O<sub>2</sub>. The decrease in absorbance at 290 nm was recorded every 20 s for 3 min. The APX activity was calculated using an extinction coefficient of 2.8 mM<sup>-1</sup> cm<sup>-164</sup>.

**SOD assay.** Total SOD activity was determined by using methods as described by<sup>65</sup>. The reaction mixture contained 50 mM phosphate buffer (pH 7.8), 0.66 mM EDTA, 10 mM methionine, 33 µM NBT, 0.0033 mM riboflavin and 50 µL cyanobacterial enzyme extract. The reaction was allowed to proceed under fluorescent illumination. After that, the absorbance of the reaction mixture was read at 560 nm. One unit of SOD activity was defined as the number of enzymes required to cause 50% inhibition of the NBT photo-reduction. The results were expressed as unit of SOD activity per mg of total soluble protein.

**Statistics.** Variance (ANOVA) and the bivariate analysis were used and Pearson's correlation method was followed to evaluate the relationship among parameters. Statistical analyses were performed with the help of IBM SPSS V25.

H<sub>2</sub>O<sub>2</sub> concentrations showed correlations with increasing PAR intensities and decreasing P concentrations independently. The fitted curve patterns were different for each PAR intensity or each P concentration.

Therefore, the most fitted curves of H<sub>2</sub>O<sub>2</sub> concentration with respect to P concentration, and with respect to PAR intensity, 30–200 µmol m<sup>-2</sup> s<sup>-1</sup>, were obtained for each PAR intensity, and the P concentration, 0.1–1000 mg L<sup>-1</sup>, respectively. Then, the effect of PAR intensity and P concentration on the H<sub>2</sub>O<sub>2</sub> concentration was estimated.

The variance (ANOVA) and the bivariate analysis were used and Pearson's correlation method was followed to evaluate the relationship among parameters. Statistical analyses were performed with the help of IBM SPSS V25.

Received: 23 June 2021; Accepted: 19 November 2021

Published online: 07 January 2022

## References

- Barrington, D. J. & Ghadouani, A. Application of hydrogen peroxide for the removal of toxic cyanobacteria and other phytoplankton from waste water. *Environ. Sci. Technol.* **4**(23), 8916–8921 (2008).
- Lurling, M., Meng, D. & Fassen, E. L. Effects of hydrogen peroxide and ultrasound on biomass reduction and toxin release in cyanobacterium, *Microcystis aeruginosa*. *Toxins* **6**(12), 3260–3281 (2014).
- Ghime, D. & Ghosh, P. Advanced oxidation processes: A powerful treatment option for the removal of recalcitrant organic compounds. In *Advanced Oxidation Processes-Applications, Trends, and Prospects* (IntechOpen, 2020).
- Rahdar, S., Igwegbe, C. A., Ghasem, M. & Ahmadi, S. Degradation of aniline by the combined process of ultrasound and hydrogen peroxide (US/H<sub>2</sub>O<sub>2</sub>). *MethodsX* **6**, 492–499 (2019).
- Derakhshan, Z. *et al.* Evaluation of kenaf fibers as moving bed biofilm carriers in algal membrane photobioreactor. *Ecotoxicol. Environ. Saf.* **152**, 1–7 (2018).
- Shekoochian, S. *et al.* Performance evaluation of cyanobacteria removal from water reservoirs by biological method. *Afr. J. Microbiol. Res.* **7**(17), 1729–1734 (2013).
- Cooper, W. J., Zika, R., Petasne, R. G. & Plane, J. M. Photochemical formation of hydrogen peroxide in natural waters exposed to sunlight. *Environ. Sci. Technol.* **22**, 1156–1160. <https://doi.org/10.1021/es00175a004> (1988).
- Cooper, W. J., Lean, D. R. S. & Carey, J. H. Spatial and temporal patterns of hydrogen peroxide in lake waters. *Can. J. Fish. Aquat. Sci.* **46**, 1227–1231. <https://doi.org/10.1139/f89-158> (1989).
- Cory, R. M. *et al.* Seasonal dynamics in dissolved organic matter, hydrogen peroxide, and cyanobacterial blooms in Lake Erie. *Front. Mar. Sci.* <https://doi.org/10.3389/fmars.2016.00054> (2016).
- Caverzan, A. *et al.* Plant responses to stresses: Role of ascorbate peroxidase in the antioxidant protection. *Genet. Mol. Biol.* **35**(4), 1011–1019 (2012).
- Sharma, P., Jha, A. B., Dubey, R. S. & Pessarakli, M. Reactive oxygen species, oxidative damage, and antioxidative defense mechanism in plants under stressful conditions. *J. Bot.* **2012**, 1–26 (2012).
- Ugya, A. Y., Imam, T. S., Li, A., Ma, J. & Hua, X. Antioxidant response mechanism of freshwater microalgae species to reactive oxygen species production: A mini review. *J. Chem. Ecol.* **36**(2), 174–193 (2020).
- Rastogi, R. P., Singh, S. P., Häder, D.-P. & Sinha, R. P. Detection of reactive oxygen species (ROS) by the oxidant-sensing probe 2',7'-dichlorodihydrofluorescein diacetate in the cyanobacterium *Anabaena variabilis* PCC 7937. *Biochem. Biophys. Res. Commun.* **397**(3), 603–607 (2010).
- Foyer, C. H. Reactive oxygen species, oxidative signaling and the regulation of photosynthesis. *Environ. Exp. Bot.* **154**, 134–142 (2018).
- Gill, S. S. & Tuteja, N. Reactive oxygen species and antioxidant machinery in abiotic stress tolerance in crop plants. *Plant Physiol. Biochem.* **48**(12), 909–930 (2010).
- Ma, Z. & Gao, K. Spiral breakage and photoinhibition of *Arthrospira platensis* (Cyanophyta) caused by accumulation of reactive oxygen species under solar radiation. *Environ. Exp. Bot.* **68**(2), 208–213 (2010).
- Welkie, D. G. *et al.* A hard day's night: Cyanobacteria in diel cycles. *Trends Microbiol.* **27**(3), 231–242 (2019).

18. Latifi, A., Ruiz, M. & Zhang, C. C. Oxidative stress in cyanobacteria. *FEMS Microbiol. Rev.* **33**(2), 258–278 (2009).
19. Lea-Smith, D. J., Bombelli, P., Vasudevan, R. & Howe, C. J. Photosynthetic, respiratory and extracellular electron transport pathways in cyanobacteria. *Biochim. Biophys. Acta (BBA) Bioenerg.* **1857**(3), 247–255 (2016).
20. Raja, V., Majeed, U., Kang, H., Andrabi, K. I. & John, R. Abiotic stress: Interplay between ROS, hormones and MAPKs. *Environ. Exp. Bot.* **137**, 142–157 (2017).
21. Asada, S., Fukuda, K., Oh, M., Hamanishi, C. & Tanaka, S. Effect of hydrogen peroxide on the metabolism of articular chondrocytes. *Inflamm. Res.* **48**(7), 399–403 (1999).
22. Nishiyama, Y. & Murata, N. Revised scheme for the mechanisms of photoinhibition and its application to enhance the abiotic stress tolerance of the photosynthetic machinery. *Appl. Microbiol. Biotechnol.* **98**(21), 8777–8796 (2014).
23. Mikula, P., Zezulka, S., Jancula, D. & Marsalek, B. Metabolic activity and membrane integrity changes in *Microcystis aeruginosa*—New findings on hydrogen peroxide toxicity in cyanobacteria. *Eur. J. Phycol.* **47**(3), 195–206 (2012).
24. Huisman, J. & Hulot, F. D. Population dynamics of harmful cyanobacteria. In *Harmful Cyanobacteria*, 143–176 (Springer, 2005).
25. Bergström, A. K. The use of TN:TP and DIN:TP ratios as indicators for phytoplankton nutrient limitation in oligotrophic lakes affected by N deposition. *Aquat. Sci.* **72**(3), 277–281 (2010).
26. Downing, J. A. & McCauley, E. The nitrogen: Phosphorus relationship in lakes. *Limnol. Oceanogr.* **37**(5), 936–945 (1992).
27. Horne, A. J. & Goldman, C. R. *Limnology* Vol. 2 (McGraw-Hill, 1994).
28. Mittler, R. Abiotic stress, the field environment and stress combination. *Trends Plant Sci.* **11**(1), 15–19. <https://doi.org/10.1016/j.tplants.2005.11.002> (2006).
29. Saints, M., Diaz, P., Monza, J. & Borsani, O. Heat stress results in loss of chloroplast Cu/Zn superoxide dismutase and increased damage to Photosystem II in combined drought-heat stressed *Lotus japonicus*. *Physiol. Plant* **140**(1), 46–56. <https://doi.org/10.1111/j.1399-3054.2010.01383.x> (2010).
30. Suzuki, N., Rivero, R. M., Shulaev, V., Blumwald, E. & Mittler, R. Abiotic and biotic stress combinations. *New Phytol.* **203**(1), 3–43. <https://doi.org/10.1111/nph.12797> (2014).
31. Asaeda, T. & Barnuevo, A. Oxidative stress as an indicator of niche-width preference of mangrove *Rhizophora stylosa*. *For. Ecol. Manag.* **432**, 73–82 (2019).
32. Asaeda, T., Senavirathna, M. D. H. J., Vamsi Krishna, L. & Yoshida, N. Impact of regulated water levels on willows (*Salix subfragilis*) at a flood-control dam, and the use of hydrogen peroxide as an indicator of environmental stress. *Ecol. Eng.* **127**, 96–102 (2019).
33. Asaeda, T., Senavirathna, M. D. H. J. & Vamsi Krishna, L. Evaluation of habitat preference of invasive macrophyte *Egeria densa* in different channel slopes using hydrogen peroxide as an indicator. *Front. Plant Sci.* **11**, 422. <https://doi.org/10.3389/fpls.2020.00422> (2020).
34. Diaz, J. & Plummer, S. Production of extracellular reactive oxygen species by phytoplankton: Past and future directions. *J. Plankton Res.* **40**(6), 655–666 (2018).
35. Drábková, M., Admiraal, W. & Maršálek, B. Combined exposure to hydrogen peroxide and PAR selective effects on cyanobacteria, green algae, and diatoms. *Environ. Sci. Technol.* **41**(1), 309–314 (2007).
36. Bouchard, J. N. & Purdie, D. A. Effect of elevated temperature, darkness and hydrogen peroxide treatment on oxidative stress and cell death in the bloom-forming toxic cyanobacterium *Microcystis aeruginosa*. *J. Phycol.* **47**(6), 1316–1325 (2011).
37. Leunert, F., Eckert, W., Paul, A., Gerhardt, V. & Grossart, H. P. Phytoplanktonic response to UV-generated hydrogen peroxide from natural organic matter. *J. Plankton Res.* **36**(1), 185–197. <https://doi.org/10.1093/plankt/ftb096> (2014).
38. Wang, B. *et al.* Optimization method for *Microcystis* bloom mitigation by hydrogen peroxide and its stimulative effects on growth of chlorophytes. *Chemosphere* **228**, 503–512 (2019).
39. Foo, S. C., Chapman, I. J., Hartnell, D. M., Turner, A. D. & Franklin, D. J. Effects of H<sub>2</sub>O<sub>2</sub> on growth, metabolic activity and membrane integrity in three strains of *Microcystis aeruginosa*. *Environ. Sci. Pollut. Res.* **27**(31), 38916–38927 (2020).
40. Barrington, D. J., Reichwaldt, E. S. & Ghadouani, A. The use of hydrogen peroxide to remove cyanobacteria and microcystins from waste stabilization ponds and hypereutrophic systems. *Ecol. Eng.* **50**, 86–94 (2013).
41. Drábková, M., Matthijs, H., Admiraal, W. & Maršálek, B. Selective effects of H<sub>2</sub>O<sub>2</sub> on cyanobacterial photosynthesis. *Photosynthetica* **45**(3), 363–369 (2007).
42. Marsac, N. T. D. Occurrence and nature of chromatic adaptation in cyanobacteria. *J. Bacteriol.* **130**(1), 82–91 (1977).
43. Garcia, P. E., Queimalinos, C. & Dieguez, M. C. Natural levels and photo-production rates of hydrogen peroxide (H<sub>2</sub>O<sub>2</sub>) in Andean Patagonian aquatic systems: Influence of the dissolved organic matter pool. *Chemosphere* **217**, 550–557 (2019).
44. Herrmann, R. The daily changing pattern of hydrogen peroxide in New Zealand surface waters. *Environ. Toxicol. Chem.* **15**(5), 652–662 (1996).
45. Spoo, L. *et al.* Elimination of cyanobacteria and microcystins in irrigation water—Effects of hydrogen peroxide treatment. *Environ. Sci. Pollut. Res.* **27**(8), 8638–8652. <https://doi.org/10.1007/s11356-019-07476-x> (2020).
46. Lopez, C. V. G. *et al.* Protein measurements of microalgae and cyanobacterial biomass. *Bioresour. Technol.* **101**(19), 7587–7591 (2010).
47. Vestervik, P. S. M., Misiorek, J. O., Spoo, L. E. M., Toivola, D. M. & Meriluoto, J. A. O. Comparative cellular toxicity of hydrophilic and hydrophobic microcystins on Caco-2 cells. *Toxins* **4**(11), 1008–1023 (2012).
48. Preece, E. P., Hardy, F. J., Moore, B. C. & Bryan, M. A review of microcystin detections in estuarine and marine waters: Environmental implications and human health risk. *Harmful Algae* **61**, 31–45 (2017).
49. Pham, T.-L. & Utsumi, M. An overview of the accumulation of microcystins in aquatic ecosystems. *J. Environ. Manag.* **213**, 520–529 (2018).
50. Goldman, J. C., McCarthy, J. J. & Peavey, D. G. Growth rate influence on the chemical composition of phytoplankton in oceanic waters. *Nature* **279**(5710), 210–215 (1979).
51. Paerl, H. W., Fulton, R. S. 3rd., Moisander, P. H. & Dyble, J. Harmful freshwater algal blooms, with an emphasis on cyanobacteria. *Sci. World J.* **1**, 76–113 (2001).
52. Xie, L., Xie, P., Li, S., Tang, H. & Liu, H. The low TN:TP ratio, a case or result of *Microcystis* blooms?. *Water Res.* **37**(9), 2073–2080 (2003).
53. Asaeda, T., Rashid, M. H. & Schoelynck, J. Tissue hydrogen peroxide concentration can explain the invasiveness of aquatic macrophytes: A modeling perspective. *Front. Environ. Sci.* **8**, 292 (2021).
54. Hesse, K., Dittman, E. & Borner, T. Consequences of impaired microcystin production for light-dependent growth and pigmentation of *Microcystis aeruginosa* PCC 7806. *FEMS Microbiol. Ecol.* **37**(1), 39–43 (2001).
55. Tilzer, M. M. Light-dependence of photosynthesis and growth in cyanobacteria: Implications for their dominance in eutrophic lakes. *N. Z. J. Mar. Freshwater Res.* **21**(3), 401–412 (1987).
56. Iwase, S. & Abe, Y. Identification and change in concentration of musty-odor compounds during growth in blue-green algae. *J. Mar. Sci. Technol.* **8**(1), 27–33 (2010).
57. Abeynayaka, H. D. L., Asaeda, T. & Kaneko, Y. Buoyancy limitation of filamentous cyanobacteria under prolonged pressure due to the gas vesicle collapse. *Environ. Manag.* **60**(2), 293–303 (2017).
58. Rippka, R., Deruelles, J., Waterbury, J. B., Herdman, M. & Stanier, R. Y. Generic assignments, strain histories and properties of pure cultures of cyanobacteria. *Microbiology* **111**(1), 1–61 (1979).
59. Jana, S. & Choudhuri, M. A. Glycolate metabolism of three submersed aquatic angiosperms during ageing. *Aquat. Bot.* **12**, 345–354 (1982).

60. Veljovic-Jovanovic, S., Noctor, G. & Foer, C. H. Are leaf hydrogen peroxide concentrations commonly overestimated? The potential influence of artefactual interference by tissue phenolics and ascorbate. *Plant Physiol. Biochem.* **40**, 501–507 (2002).
61. Cheeseman, J. M. Hydrogen peroxide concentrations in leaves under natural conditions. *J. Exp. Bot.* **57**(10), 2435–2444 (2006).
62. Queval, G., Hager, J., Gakiere, B. & Noctor, G. Why are literature data for H<sub>2</sub>O<sub>2</sub> contents so variable? A discussion of potential difficulties in the quantitative assay of leaf extracts. *J. Exp. Bot.* **59**(2), 135–146. <https://doi.org/10.1093/jxb/erm193> (2008).
63. Aebi, H. Catalase in vitro. *Methods Enzymol.* **105**, 121–126 (1984).
64. Nakano, Y. & Asada, K. Hydrogen peroxide is scavenged by ascorbate-specific peroxidase in spinach chloroplasts. *Plant Cell Physiol.* **22**(5), 867–880 (1981).
65. Ahmad, P., Jaleel, C. A., Salem, M. A., Nabi, G. & Sharma, S. Roles of enzymatic and non enzymatic antioxidants in plants during abiotic stress. *Crit. Rev. Biotechnol.* **30**(3), 161–175 (2010).

## Acknowledgements

This work was financially supported by the Grant-in-Aid for Scientific Research (B) (19H02245) and the Fund for the Promotion of Joint International Research (18KK0116) of the Japan Society for the Promotion of Science (JSPS).

## Author contributions

T.A. contributed to the design of the experiment, analyses, and writing the manuscript. M.R. contributed to the revision of the manuscript. H.D.L.A. carried out the experiment and writing the experiment part.

## Competing interests

The authors declare no competing interests.

## Additional information

**Correspondence** and requests for materials should be addressed to T.A.

**Reprints and permissions information** is available at [www.nature.com/reprints](http://www.nature.com/reprints).

**Publisher's note** Springer Nature remains neutral with regard to jurisdictional claims in published maps and institutional affiliations.



**Open Access** This article is licensed under a Creative Commons Attribution 4.0 International License, which permits use, sharing, adaptation, distribution and reproduction in any medium or format, as long as you give appropriate credit to the original author(s) and the source, provide a link to the Creative Commons licence, and indicate if changes were made. The images or other third party material in this article are included in the article's Creative Commons licence, unless indicated otherwise in a credit line to the material. If material is not included in the article's Creative Commons licence and your intended use is not permitted by statutory regulation or exceeds the permitted use, you will need to obtain permission directly from the copyright holder. To view a copy of this licence, visit <http://creativecommons.org/licenses/by/4.0/>.

© The Author(s) 2022